Adaptive UWB-OFDM Synthetic Aperture Radar

Md Anowar Hossain*, Ibrahim Elshafiey*, Majeed A. Alkanhal*, and Ahmed Mabrouk**
* Electrical Engineering Dept. and Prince Sultan Advanced Technologies Research Institute (PSATRI)
King Saud University
Riyadh, Kingdom of Saudi Arabia
E-mail: anwar_cce@yahoo.com
** Computer Science Department
International Islamic University Malaysia
Kuala lumpur, Malaysia

Abstract—**This paper presents an empirical study of high resolution potentially jamming-resistant Synthetic Aperture Radar (SAR) system based on UWB-OFDM architecture. The Range-Doppler Algorithm (RDA) was used to construct a high resolution SAR image for simulation purpose. Suitable waveforms to achieve high resolution SAR imaging are proposed for both friendly and hostile environments. The proposed waveforms were tested for a point scatterer and for full 2-D SAR image construction. Simulation results demonstrate the benefits of using UWB-OFDM waveforms for SAR system, such as dynamic spectrum allocation, anti-jamming potential through pulse diversity-while having a potential to produce high resolution target images. The use of UWB-OFDM waveform for SAR system proves useful for high resolution image data collection for civilian purposes and provides significant anti-jamming capabilities for military purposes.**

Keywords- Ultra-Wideband (UWB); Orthogonal Frequency Division Multiplexing (OFDM); Synthetic Aperture RADAR (SAR); Anti-jamming; High Resolution (HR).

I. INTRODUCTION

The principle idea behind Synthetic Aperture RADAR (SAR) stems from the desire for High Resolution (HR) images. SAR imaging is commonly used when general information about a broad target area is required. It involves transmitting signals at spaced intervals called Pulse Repetition Interval (PRI). The responses at each PRI are collected and processed to reconstruct a RADAR image of the terrain. HR SAR imaging is a crucial component of reconnaissance and surveillance operations for civilian and military purposes [1]. In general, HR SAR images in range dimension can be generated using ultra-wideband (UWB) waveforms for RADAR signal transmission. Often, wide bandwidths of RADAR waveforms were formed by employing ultra-short Gaussian pulse, Linear Frequency Modulation (LFM) chirp and UWB noise as RADAR signal. However, these RADARs have certain limitations such as constant pulse shape and low spectral efficiency. Therefore, it is necessary to develop RADAR signals that employ wide bandwidths to achieve HR images and at the same time have the ability to quickly adapt to any potential adverse situation such as jamming scenarios i.e. hostile environments. UWB is a wireless technology that transmits extremely low power signal over a wide swath of radio spectrum. UWB technology has double advantages: good capacity of penetration and high resolution for RADAR applications [2]. Orthogonal Frequency Division Multiplexing (OFDM) is a signal modulation scheme which is commonly utilized in commercial communications, shows great potential for use as a RADAR waveform. An OFDM signal is comprised of several orthogonal sub-carriers that are simultaneously emitted over a single transmission path. Each subcarrier occupies a small slice of the entire signal bandwidth. The system has control over the subcarriers, and therefore, control over the spectrum of the waveform [3]. In RADAR scenarios, the spectrum can be manipulated to avoid any interference that may be introduced from hostile or friendly systems. Because the signal is implemented digitally, the bandwidth of the signal will be determined by the sampling rate of the Digital-to-Analog Converter (DAC). Advances in sampling technology have increased sampling speed allowing for OFDM waveforms employing UWB (500 MHz and above) to be generated accurately and at relatively low costs. The result is a diverse signal capable of HR imaging.

Although OFDM has been elaborately studied and commercialized in the digital communication field, it has not so widely been studied by RADAR communities apart from a few efforts [4] and [5]. Garmatyuk first introduced OFDM based SAR imaging and provided a proof of concept based on Back-projection algorithm [6]. Our work aimed at providing the high resolution SAR image reconstruction based on Range Doppler Algorithm (RDA) to achieve accuracy in matching the exact SAR transfer function [7]. The proposed system is able to adapt with both friendly and hostile environment by using two distinct UWB-OFDM waveforms while having the same architecture.

II. SYSTEM DESCRIPTION

Figure 1 shows the block diagram of a UWB-OFDM SAR. A switch first determines whether a random or pseudo-random binary source will be used to generate the signal. The samples are then sent to an Inverse Fast Fourier Transform (IFFT) processor to convert the signal to time domain where each samples represent a sub-band of the OFDM signal. The elements are sent one at a time to the DAC (1Gs/s) to generate the analog UWB-OFDM signal having baseband bandwidth of 500 MHz. The output of

This research work is supported by the National Plan for Science and Technology, Kingdom of Saudi Arabia, under project no: ELE262-2-08

978-1-4577-0069-9/11/$26.00 ©2011 IEEE

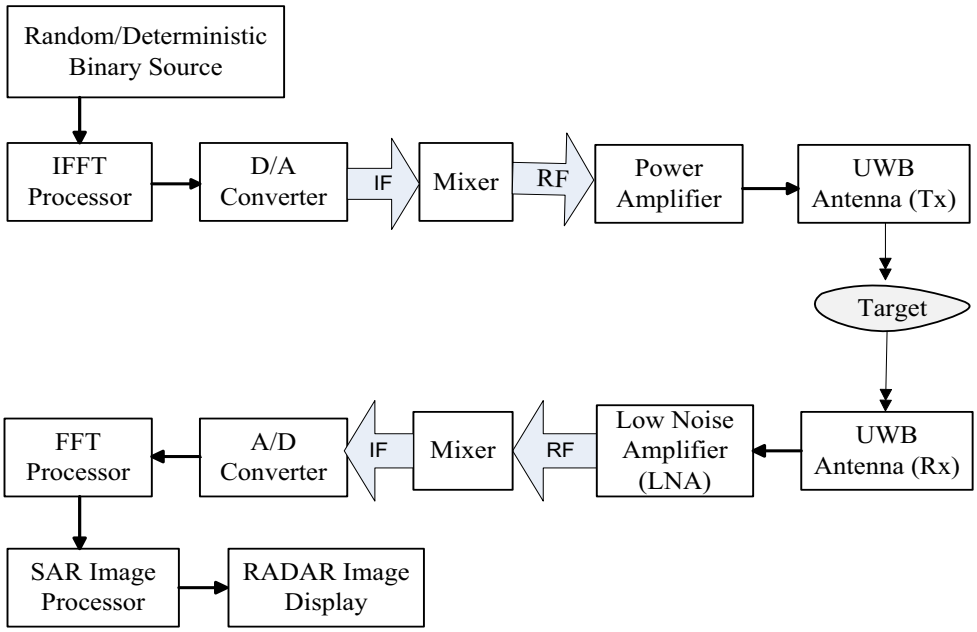

Figure 1. Block diagram of a UWB-OFDM SAR

DAC is heterodyned with a free running oscillator (mixer) at a frequency of 7.5 GHz, the result of which is the continuous time UWB-OFDM signal. The signal would then pass through a power amplifier and finally transmitted through a UWB antenna (Tx). Any reflected signal from targets is received by another UWB antenna (Rx) and amplified by a Low Noise Amplifier (LNA). LNA is usually located very close to the detection device (antenna) to reduce losses in the feedline. The signal is again heterodyned and reduced to baseband. The baseband signal is then sampled by an Analog-to-Digital Converter (ADC) that samples at rate (1Gs/s) equal to the DAC. The output of the ADC is then fed to FFT processor to convert samples to frequency domain the result of which is raw data. Post processing is then performed on raw data to display the RADAR image.

III. UWB-OFDM SIGNAL CONSTRUCTION

Simulation of an OFDM signal is performed by randomly or pseudo-randomly populating the digital frequency domain vector as [8]:

$$S_{\omega} = \left[X_{ns} 0 X_{ps} \right] \tag{1}$$

Where, X_{ps} and X_{ns} represent the positive and negative sub-band (flipped version of X_{ps}) respectively whereas 0 represents the DC value. If we consider ON-OFF keying which is a special case of Amplitude Shift Keying (ASK) then a 1 in vector X_{ps} means the sub-band exists in the signal and is deemed 'ON'. On the other hand, a 0 in vector X_{ps} means that the sub-band is deemed 'OFF' as described in [6]. IFFT is then applied to S_{ω} to get the discrete time domain OFDM signal as:

$$S_{tx} = F^{-1}\left[S_{\omega} \right] \tag{2}$$

The signals in Fig. 2 and Fig. 3 are generated using the following parameters: number of sub-bands = 128, sampling time, Δt_s = 1ns results in baseband bandwidth, $B_0 = 1/2\Delta t_s$ = 500 MHz, dividing by a factor of two to satisfy Nyquist criterion.

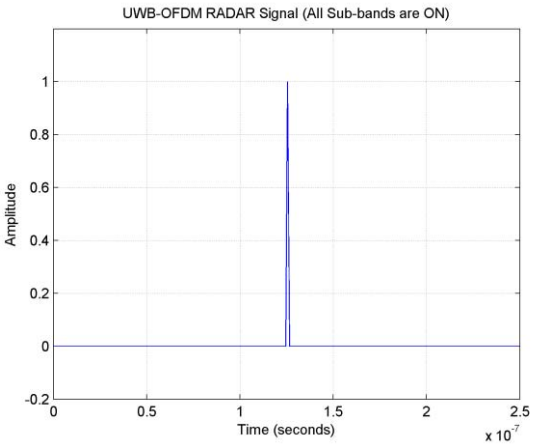

Figure 2. UWB-OFDM RADAR Signal (All sub-bands are 'ON')

Observing Fig. 2 we see that when all sub-bands are 'ON' the UWB-OFDM waveform becomes a short spike with a width equal to $2\Delta t_s$ which will give the best possible range resolution and exact location of the target. We can consider this signal for the system in friendly environment to achieve HR images. However, the pulse is not unique which will cause the system to suffer in hostile environment. Fig. 3 shows an UWB-OFDM waveform when X_{ps} populated randomly with 1's and 0's. We can observe that the signal is noise-like and it gives a unique signal at each PRI, which will bode well for the SAR system in jamming scenarios i.e. hostile environment. The system can be adapted with both environments just by changing the transmitted waveforms.

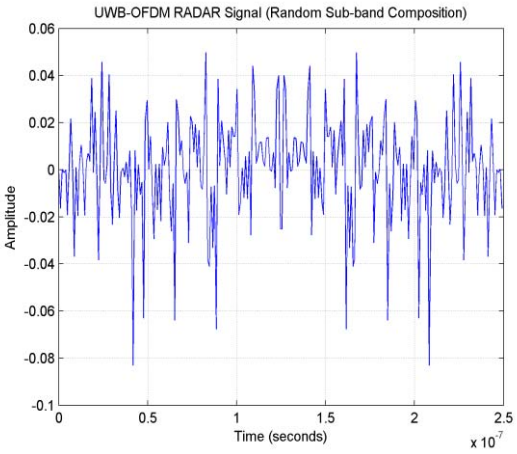

Figure 3. UWB-OFDM RADAR Signal (Random sub-band composition)

The difficulty of intercepting OFDM signal in comparison with Linear Frequency Modulated (LFM) chirp signal is illustrated by using simple spectrogram approach [9]. Both signals are generated in baseband, as it is assumed that jammer knows the center frequency transmitted waveform and is capable of removing it to predict the RADAR transmitted signal.

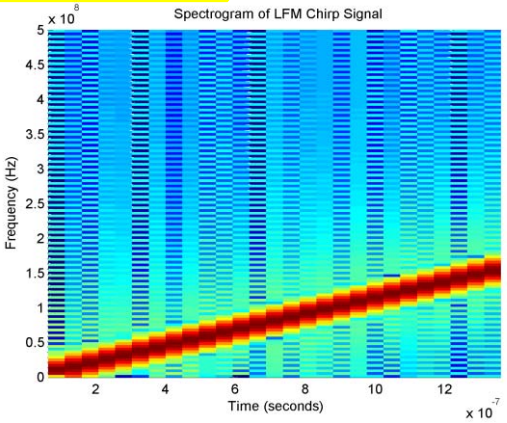

Figure 4. Spectrogram of LFM Chirp Signal

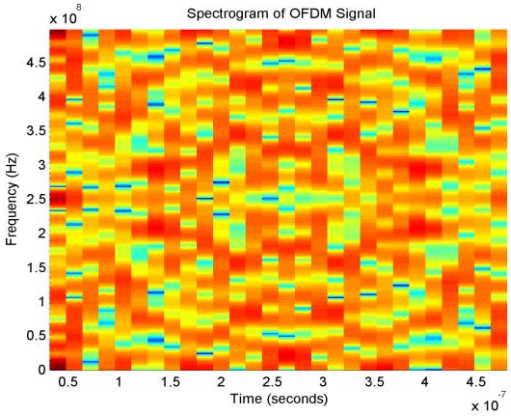

Figure 5. Spectrogram of UWB-OFDM Signal

It is clear that the time-frequency behavior of LFM chirp signal is easy to predict and intercept because of the linear nature of Instantaneous Frequency (IF) as shown in Fig. 4. On the other hand, OFDM waveform with random sub-band distribution is evidently hardest to predict as shown in Fig. 5. This is due to the fact that the signal is inherently multi-frequency.

IV. RANGE IMAGING

Let us consider a point target reflection located at some range, R=15 meters. The expected received RADAR signal as shown in Fig. 6 is a truncated time delayed version of transmitted signal (S_{tx}) and has the form

$$S_{rx}(t) = S_{tx}(t - t_d) \quad \text{Where, } t_d = \frac{2R}{c} \tag{3}$$

t_d is the time delay introduced by the target and c is the velocity of light. The truncation of the received signal, $S_{rx}(t)$ comes from the fact that the beginning of the swath represents $t=0$, the time when signal sampling begins, at which point ADC will acquire all samples. Only when the ADC samples for at least t_d, then $S_{rx}(t)$ begin being sampled.

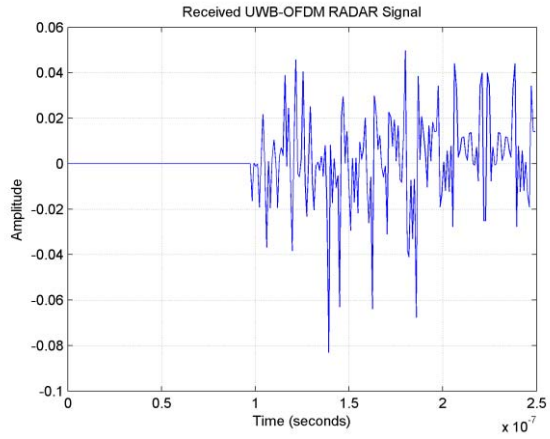

Figure 6. Received UWB-OFDM RADAR Signal

We then apply match filtering in frequency domain and convert the signal to time domain to resolve the target as

$$S_{Mx}(t) = F^{-1}\left[S_{rx}(\omega) S_{tx}^{*}(\omega)\right] \tag{4}$$

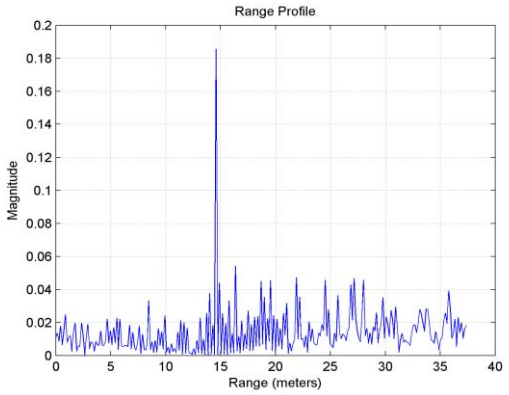

Figure 7. Range Profile (Point target resolved at 15 meters)

Figure 7 shows the range profile with resolved point target located at 15 meters. The range profile is generated by changing $S_{Mx}(t)$ to $S_{Mx}(x)$ using $t=2x/c$. The range resolution

can be calculated as $\Delta R = c/2B_0 = 0.30$ meters. Although the side-lobes are approximately 12dB, reasonable side-lobes of 35 to 40 dB can be achieved by increasing sub-band fill ratio i.e. more than 60% of total sub-band should be turned 'ON'.

V. CROSS-RANGE IMAGING AND FULL 2-D SAR IMAGE RECONSTRUCTION

Imaging in the direction parallel to the movement of the RADAR platform is performed in slow-time domain. Stripmap SAR topology shown in Fig. 8 was assumed to perform the cross-range imaging and full image reconstruction.

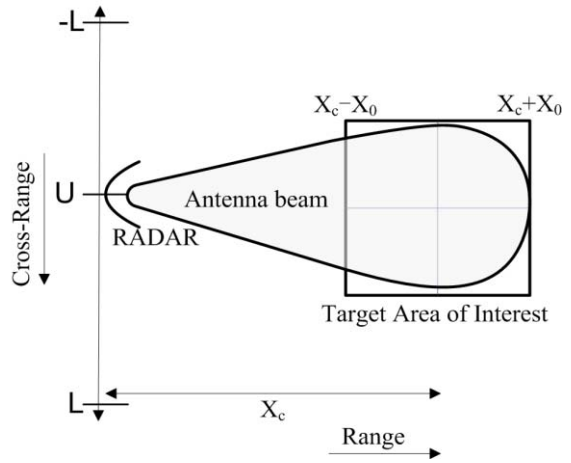

Figure 8. Stripmap SAR Topology

The signal shown in Fig. 2 was used as transmitted pulse to achieve high resolution image. Table I shows the parameters used in simulation.

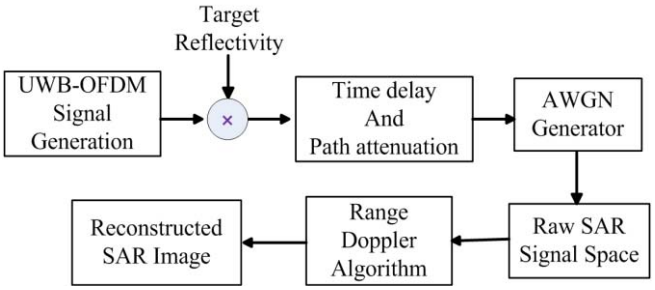

Figure 9. Simulation Model

Figure 9 shows the system model used for simulation purpose. At each synthetic aperture position (u), an UWB-OFDM signal is transmitted. The time-delayed and attenuated received signal are stored so that after the final transmitted and received signal there exist a matrix containing received signals for each synthetic aperture position. The received signal is given by

$$S_{rx}(t,u) = \sum_{n=1}^{N} \sigma_n S(t - t_{dn})$$

(5)Where, N, σ_n and t_{dn} are number of targets, target reflectivity and round-trip time associated with n[th] target.

The delay t_{dn} is given by

$$t_{dn} = \frac{2}{c}\sqrt{(X_c + x_n)^2 + (u + y_n)^2} \quad (6)$$

Where, X_C is the range distance to the center of the target area and (x_n, y_n) is the position of nth target. Multiplying equation (5) by $e^{-j\omega t_{dn}}$, we convert the received signal, $S_{rx}(t,u)$ to the baseband representation to generate the raw data and obtain received phase history as

$$S_{rx}(\omega,u) = e^{-j\omega t_{dn}} \sum_{n=1}^{N} \sigma_n S(t - t_{dn}) \quad (7)$$

TABLE I. UWB-OFDM SAR SIMULATION PARAMETERS

Parameter	Symbol	Value
Pulse Repetition Frequency	PRF	300 Hz
Duration of Flight	Dur	3 seconds
Velocity of the platform	V_P	200 m/s
Carrier Frequency	f_c	7.5 GHz
Half Target Area Width	X_0	200 m

For simplicity, we will start by assuming a single point scatterer. Fig. 10 shows the raw data generated by assuming a single point target at $(x_n, y_n) = (0, 0)$.

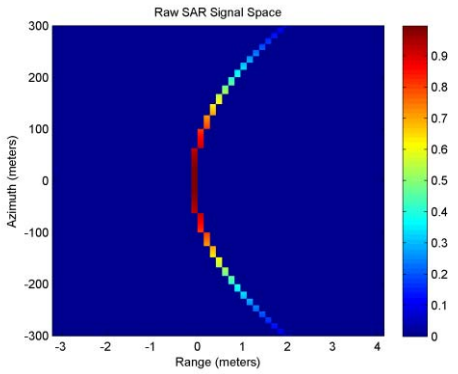

Figure 10. Raw SAR signal space

Now we can implement RDA to resolve the target. For range compression as shown in Fig. 11, we have to perform match filtering between raw data and range reference signal as

$$S_{Mx}(t,u) = F^{-1}\left[S_{rx}(\omega,u) S^*_{tx0}(\omega,u)\right] \quad (8)$$

The range reference signal $S_{tx0}(\omega,u)$ is an ideal echo signal from a unit reflector at the center of the current range swath and is given by

$$S_{tx0} = S(t - t_{d0}) \quad \text{Where, } t_{d0} = \frac{2X_c}{c} \quad (9)$$

Range Cell Migration Correction (RCMC) is needed to capture all the signal energy for azimuth compression and to remove the hyperbolic trend w.r.t. azimuth time of the instantaneous slant range causing Range Cell Migration (RCM) is calculated as

$$\Delta R = \left(\sqrt{X_c^2 + u^2}\right) - X_c \tag{10}$$

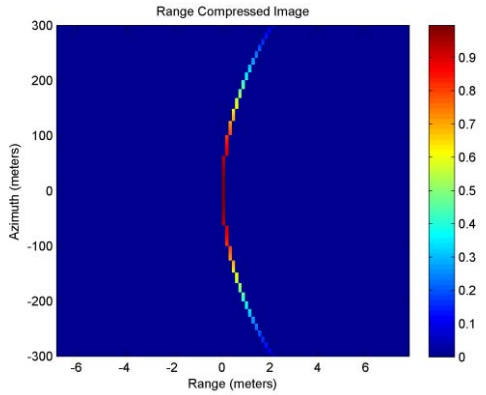

Figure 11. Image after range compression

RCM is rounded to the nearest integer after dividing by the cell size as the migration must be calculated in discrete cells to be corrected during RCMC process. The cells are shifted to counter RCM to perform RCMC as shown in Fig. 12 prior to azimuth (cross-range) compression. The cell size is calculated as

$$\Delta X = \frac{c\Delta t_s}{2} \tag{11}$$

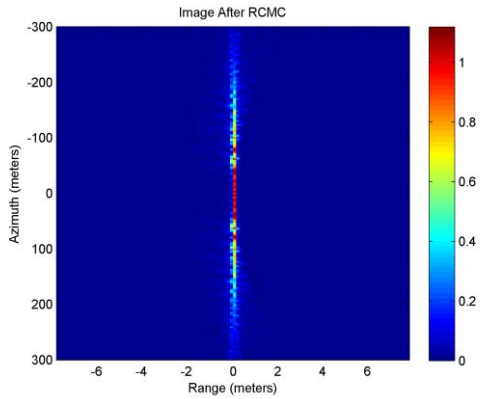

Figure 12. Image after RCMC

For azimuth compression, azimuth match filtering must be performed in frequency domain between signals after RCMC and azimuth reference signal. IFFT is then performed to reconstruct the final SAR image. The azimuth reference signal is defined as an ideal return from a unit reflector located at the center of RADAR-scanned target area-i.e. (x_n, y_n) = (X_C, 0) and is given as

$$S_0(\omega, u) = e^{-j\frac{2\omega}{c}\sqrt{X_c^2+u^2}} \tag{12}$$

Fig. 13 shows the reconstructed SAR image of a point target at the position (x_n, y_n) = (0, 0).

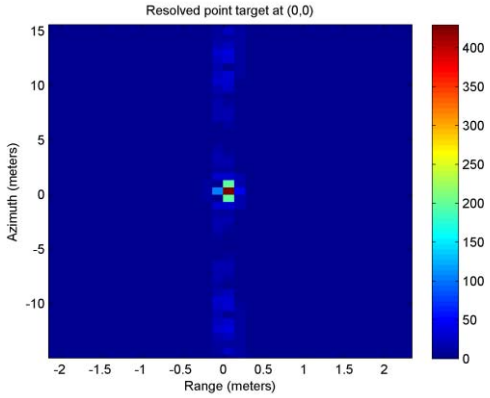

Figure 13. Resolved point target at (x_n, y_n)=(0, 0)

In jamming scenarios, The RADAR signal is replicated and delayed to create a false range offset. The delayed signal is transmitted at the next expected arrival of the RADAR signal and is seen as an actual target during the correlation process. The jammer transmitted jammer signal (received signal for RADAR) is given as

$$J_{tx}(t,u) = S_{txj}\left(t - t_{dj}\right) \tag{13}$$

where, $t_{dj} = \frac{2}{c}\sqrt{(X_c + x_j)^2 + (u + y_j)^2}$ denotes the jammer introduced time delay and (x_j, y_j) is the position of the false target. Under the assumption that center frequency is known to the jammer and it could form exact replicas of the transmitted SAR signal, the RADAR received signal in jamming scenarios is given by

$$S_{rxj}(t,u) = \sum_{n=1}^{N} \sigma_n S\left(t - t_{dn}\right) + J_{tx}(t,u) \tag{14}$$

Point target is also reconstructed by using noise-like UWB-OFDM waveform shown in Fig. 3 as a transmitted pulse in jamming scenarios.

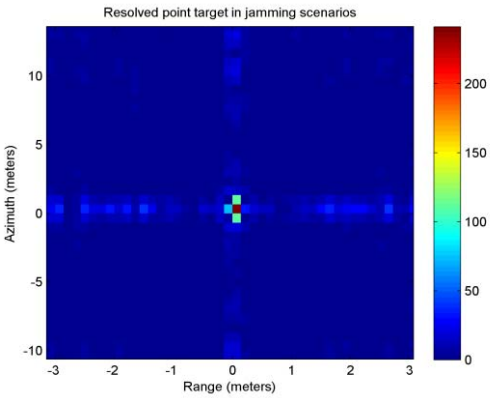

Figure 14. Resolved point target in jamming scenarios

Fig. 14 shows the resolved point target using a fresh waveform at each PRI. Because of transmitting a unique UWB-OFDM signal at each PRI, the signal has weaker

correlation with the jammer signals causing no false target appears in the reconstructed SAR image. The target is still fairly visible in presence of some ambiguities.

Full image reconstruction is performed using a gray scale image of a 'tank' as a target profile. The input image is converted to a 2-D matrix and the values of each element were normalized to use as reflectivity. The positions of the columns and rows for each element are assumed as range and cross-range of the targets.

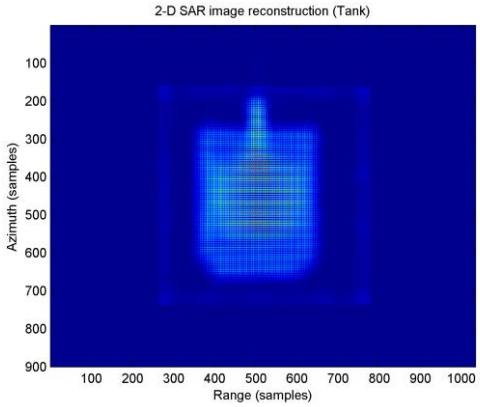

Figure 15. Full 2-D SAR image reconstruction

Fig. 15 shows that the full 2- D reconstructed SAR image of a 'tank'. However, the trade-off is greater computation time when using an image as a target profile.

Full image reconstruction is also performed by considering jamming scenarios as shown in Fig. 16, transmitting a unique UWB-OFDM pulse at each PRI. Automatic Target Recognition (ATR) is still possible with negligible ambiguities in the reconstructed SAR image.

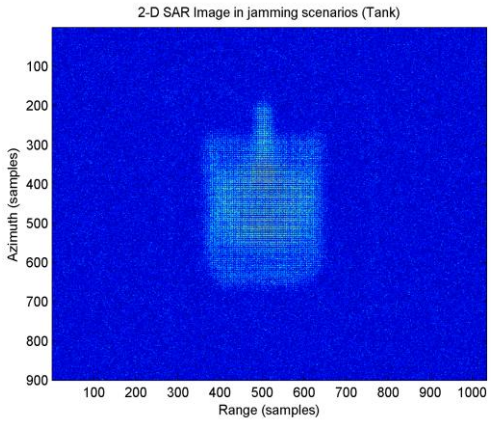

Figure 16. 2-D SAR image reconstruction in jamming scenarios

VI. CONCLUSION

Performance of UWB-OFDM based SAR imaging has been investigated for both friendly and hostile environment. The anti-jamming capabilities of UWB-OFDM waveform was addressed in comparison with LFM chirp signal. Simulation result shows that UWB-OFDM waveform behaved remarkably well against jammers. UWB technique improves the resolution of SAR image in range domain. The resolution of the proposed SAR system can be enhanced just by replacing the DAC and ADC with higher sampling speed.

REFERENCES

[1] M. Soumekh, *Synthetic Aperture Radar Signal Processing with MATLAB Algorithms*, 2nd ed. New York, United States of America: Wiley, 1999.

[2] R. Aiello and S. Wood, *Essentials of UWB*, 1st ed. New York: Cambridge, 2008.

[3] L. Hanzo and T. Keller, *OFDM and MC-CDMA*, 2nd ed. West Sussex, United Kingdom: Wiley, 2006.

[4] D. Garmatyuk and K. Kauffman, "Radar and data communication fusion with UWB-OFDM software-defined system," in *Proc. of IEEE int. conf. Ultra-Wideband,* Vancouver, BC, Canada, 2009, pp. 454-458.

[5] D. Garmatyuk, K. Kauffman, J. Schuerger, and S. Spalding, "Wideband OFDM system for radar and communications," in *Proc. of IEEE Radar Conf.*, Pasadena, CA, 2009, pp. 1-6.

[6] D. Garmatyuk et al., "Feasibility study of a multi-carrier dual-Use imaging radar and communication system," in *Proc. of 37th European Microwave Conf.*, Munich, 2007, pp. 1473-1476.

[7] Yew L. Neo, Frank H. Wong, and Ian G. Cumming, "Processing of azimuth-invariant bistatic SAR data using the range doppler algorithm," *IEEE Trans. on Geosc. Rem. Sens.*, vol. 46, no. 1, pp. 14-21, Jan. 2008.

[8] H. Schulze and C. Luders, *Theory and Applications of OFDM and CDMA*, 2nd ed. New York, USA: John Wiley & Sons, 2001.

[9] *Spectrogram* (Signal Processing ToolBox), MATLAB 2010, The Mathworks Inc.